

Combined use of high spatial resolution optical and radar satellite data for the monitoring of wheat crops in the semi-arid Tensift/Marrakech plain

Hadria R.¹, B. Duchemin², F. Baup², I. Benhadj², G. Boulet², A. Bouvet², G. Dedieu², J. Ezzahar¹, O. Hagolle², L. Jarlan², S. Khabba¹, M. Lepage², A. Olioso³, T. LeToan²

¹ Faculté des Sciences Semlalia, Université Cadi Ayyad, Avenue Prince My Abdellah, BP 2390, Marrakech, Maroc

² CESBIO – Centre d'Etudes Spatiales de la Biosphère, 18 Avenue Edouard Belin, bpi 2801, 31401, Toulouse cedex 9, France

³ INRA / université d'Avignon, UMR1114, Environnement Méditerranéen et Modélisation des Agro-Hydrosystèmes, Domaine Saint-Paul, Site Agroparc, F-84914 Avignon, France, Avignon, France

Abstract

In this study, we investigated the potential of FORMOSAT-2 and ENVISAT/ASAR for the monitoring of irrigated wheat crops over a 10 km² semi-arid area located in the Tensift/Marrakech plain. These satellite are designed to provide both high spatial resolution (10 m) and frequent (daily) time of revisit. The FORMOSAT-2 Taiwanese satellite (<http://www.nspo.org.tw>) can provide 8m resolution images every day in 4 bands ranging from blue to near-infrared spectral domains. The Advanced Synthetic Aperture Radar (ASAR), onboard ENVISAT mission (<http://envisat.esa.int/>) operates in the C-band a spatial resolution of about 30m in the Alternating Polarisation mode. The orbital cycle of ASAR is 35 days, but the combination of acquisitions with different incidence and path configurations allows a revisit time of a few days.

The experiment was set up during the 2005-2006 wheat agricultural season on an irrigated area located at 40 km East of Marrakech. This semi-arid area was intensively monitored as part of the SudMed program (<http://www.irrimed.org/irri&sudmed.htm>). The experimental data set includes information on agricultural practices, vegetation biophysical variables (green leaf area index and dry aerial mass of canopies). FORMOSAT-2 images were programmed with a nominal time step of 4 days and about 25 cloud-free images were acquired during the 2005-2006 agricultural season (November to May). 15 ASAR Alternating Polarisation images were available at the same period, all. The images were all acquired in ascending pass at high incidence angles (35° to 45°) in dual polarisations (VV and HH).

We first used the time series of FORMOSAT-2 images acquired during the 2005/2006 agricultural season to characterise the vegetation dynamics. Green leaf area index was inverted from Vegetation Indices derived from FORMOSAT-2 images with a 25% accuracy. In a second step, this information was incorporated into a canopy functioning/water balance model to provide spatial estimates of green leaf area index, dry aerial biomass and top-soil moisture. These outputs were evaluated at the field scale using data collected at ground on 8 wheat fields. The model accurately simulates the time courses of leaf area index and dry aerial mass during the vegetative phase (20% error). Finally, we analysed the spatio-temporal variations of ASAR backscattering coefficients on the basis of these simulations. In the conditions that prevail in this study, the sensitivity of ASAR data to the vegetation density appears very low and restricted to very specific soil/plant conditions (wet soil/tillering phase).

I. Introduction

Half of the world food production originates from irrigated and drained soils on about 20% of cultivated lands (FAO/IPTRID 1999, Bastiaanssen et al. 2007). However, serious water shortages occur in arid and semi-arid areas as existing resources reach full exploitation. The design of tools providing with regional estimates of water balance and crop yield is necessary to ensure a sustainable development of these areas.

Crop simulation models are designed to describe the effect of climate, soil and agricultural practices on crop growth and production. Although models performances have continuously made progresses over the past few years, regional applications for the monitoring of water and vegetation resources are limited (Boote et al. 1996, Moulin et al. 1998, Faivre et al. 2004, Bastiaanssen et al. 2007). Indeed, shortage of geolocated data prevents the use of crop models over large areas. In particular, there are generally a large number of model parameters compared to the amount of observation available for their identification over each agricultural unit (field). Furthermore, it is difficult to cope with the lack of adequate and sufficient input data to run the model at a regional scale. This is particularly true for the information about technical practices such sowing, irrigation and fertilisation schedules, which know large space time variations. Thus, prior (imperfect) information on parameters and inputs is required resulting in simulation errors and reduction of the predictive capacity of models. As a substitute, the scientific community has investigated remotely-sensed data to provide spatial estimates of crop yield (Moulin et al. 1998, Guérif and Duke 2000, Lobell et al. 2003, Oliso et al. 2005, Mo et al. 2005, Houlès et al. 2007, Ortiz-monasterio and Lobell 2007, Tasumi and Allen 2007, Duchemin et al. 2008a).

In this context, Earth Observation Systems designed to provide both high spatial resolution (10 m) and frequent (daily) time of revisit offer strong opportunities. At the present time, two of them appear of particular interest: 1) the FORMOSAT-2 Taiwanese satellite (<http://www.nspo.org.tw>), which can provide high spatial resolution (8m) images every day in 4 bands ranging from blue to near-infrared spectral domains ; 2) the Advanced Synthetic Aperture Radar (ASAR), onboard ENVISAT mission (<http://envisat.esa.int/>), which operates in the C-band with 7 different incidence angles between 15 and 45 degrees at a spatial resolution of about 30m in the Alternating Polarisation mode. The orbital cycle of ASAR is 35 days, but the combination of acquisitions with different incidence and path configurations allows a revisit time of a few days. Optical data have been intensively used in the context of farm management (e.g. Scotford and Miller 2005). In contrast, there is a poor understanding of the radar response to agricultural soil and plant conditions (Moran et al. 2002).

In this study, we investigated the potential of FORMOSAT-2 and ASAR data for the monitoring of irrigated wheat crops over a 10 km² semi-arid area located in the Tensift/Marrakech plain. We first used a time series of FORMOSAT-2 images acquired during the 2005/2006 agricultural season to characterise the vegetation dynamics. In a second step, this information is incorporated into a canopy functioning/water balance model to provide spatial estimates of green leaf area index, dry aerial biomass and top-soil moisture. These outputs are evaluated at the field scale using data collected at ground on 8 wheat fields. Finally, we capitalize on the knowledge of plant/soil conditions in order to interpret radar images, using simulations of green leaf area index and topsoil moisture to analyse the spatio-temporal variations of ASAR backscattering coefficients.

II. Materials and methods

II.1. Study area

The experiment was set up during the 2005-2006 wheat agricultural season on an irrigated area located at 40 km East of Marrakech. This area was intensively monitored as part of the SudMed program (Benhadj et al. 2007; Chehbouni et al. 2007; Duchemin et al. 2005, 2006, 2008a, 2008b; Hadria et al. 2006, 2007; Er-Raki et al. 2007). It covers about 2800 ha and is almost flat (slope less than 1%), with deep soil of xerosol type and a fine, clay to loamy, texture.

Land-use information and soil management practices were collected on numerous fields within the study area. The dominant crops are cereals, mainly wheat. The wheat is generally sown between mid November and mid January; it reaches its peak of growth between mid-March and Mid-April; and the harvest occurs in May-June.

The experimental data set includes information on agricultural practices (ploughing, sowing, irrigation, fertilisation, weed and pest controls) for about 70 wheat fields. Amongst them, 8 test fields were sampled to estimate biophysical variables following the protocols described in Duchemin et al. (2006) and Hadria et al. (2007): the green leaf area index was measured at the end of March, and dry aerial biomass was collected at the same time and just before harvest. These variables were measured on 3 samples of 1m² for each of the 8 test fields.

Climate is basically of semi-arid continental type. Climatic data were measured by a meteorological station installed at the center of the study area, and five rain gauges of the ORMVAH network located in the vicinity of the study area. The beginning of the 2005-2006 agricultural season was very dry, with only two minor rainfall events (10-15mm) mid- and end-November, after which no rain was recorded until December 21, 2005. In contrast, the season was exceptionally wet in January and February (accumulated rainfall about 200mm), then no rain was observed in March and April. As a consequence, irrigation water was mainly supplied from mid-March to the beginning of May, and mid-December in a less extent.

II.2. FORMOSAT-2 images

FORMOSAT-2 has been launched by the National Space Organization of Taiwan (NSPO, <http://www.nspo.org.tw/>, <http://www.spot-image.com>). It is operational since May 2004 onto a sun-synchronous orbit, with onboard the Remote Sensing Instrument (RSI). RSI provides high spatial resolution images (8m in the multispectral mode for nadir viewing) in 4 narrow spectral bands ranging from 0.45 μm to 0.90 μm (blue, green, red and near-infrared). Unlike other systems operating at high spatial resolution, FORMOSAT-2/RSI observes a particular area every day with the same viewing angle. However, it only surveys a part -about the half- of the Earth.

The FORMOSAT-2 images used in this study have been collected from November 2005 to May 2006 (see Duchemin et al. 2008b). The images were programmed with a nominal time step of 4 days and about 50 images were acquired during this 7-month period of interest. 24 images were eliminated because they were contaminated by clouds. All images were acquired with an off-nadir angle of $18^{\circ}\pm 1^{\circ}$, viewing to the west across track. The images were georeferenced using an autocorrelation algorithm and a set of ground control points collected with GPS. Accuracy in geolocation was estimated to about half-pixel (4 m). The atmospheric correction was performed using the SMAC code (Rahman and Dedieu 1994) with

atmospheric water vapour content and aerosol optical depth collected by CIMEL sunphotometers installed in the vicinity of the study area. The quality of atmospheric correction is discussed in [Hagolle et al. \(2008\)](#). This processing provided us with 26 images of surface reflectances, from which two vegetation indices were calculated: (1) the Ratio Vegetation Index (RVI), which is simply the ratio of near infrared to red reflectances, (2) the Normalised Difference Vegetation Index (NDVI), defined as the difference between near infrared and red reflectances divided by their sum. The two indices were suggested by [Rouse et al. \(1974\)](#). These indices were tested against ground measurement to estimate green leaf area index from FORMOSAT-2 images.

II.3. ENVISAT/ASAR data

The Advanced Synthetic Aperture Radar (ASAR), onboard the ENVISAT mission (<http://envisat.esa.int/>) launched in March 2002, operates at C-band (frequency 5.33 GHz, wavelength 5.6 cm) with 7 different incidence angles between 15 and 45 degrees at a spatial resolution of about 30 m in the Alternating Polarisation mode. The revisit time for a given configuration of incidence angle and orbit pass is 35 days, but the combination of different incidences allows to increase the repetitivity of observations (e.g. 10 passes during the 35-day orbital cycle at 45° latitude).

Between December 2005 and May 2006, 15 ASAR Alternating Polarisation images were acquired, all in ascending pass. The images were acquired at high incidence angles (IS5 to IS7, 35.8° to 45.2° incidence angle), for which the sensitivity to vegetation is maximal ([Mattia et al., 2003](#); [Brown et al., 2003](#)). The images were acquired in dual polarisations (VV and HH) at a spatial resolution of about 30 m (12.5 m pixel size). Radiometric calibration was performed following the procedure specified by the European Space Agency ([Rosich and Meadows 2004](#)). All the images were superimposed using an automatic correlation algorithm based on contrasted objects visible in the images, then the images were co-registered on FORMOSAT-2 data using image-to-image correction. Accuracy in coregistration was estimated to about 1 pixel (12.5m). Finally, a spatio-temporal filter was applied to reduce speckle effects. The filter is described in [Lopes et al. \(1993\)](#), [Le Toan et al. \(1997\)](#), and [Quegan and Yu \(2001\)](#).

II.4. Soil/plant modelling

The SAFY ‘Simple Algorithm For Yield estimate’ is a canopy functioning model developed by [Duchemin et al. \(2008a\)](#). It includes three sub-sets of equations to simulate the time courses of total/green leaf area index (TLA/GLA), dry above-ground mass (DAM), and Grain Yield (GY). The model simulates these variables with no explicit account of water and nutrients. It only requires climatic forcing variables (daily incoming global radiation and daily average air temperature) as an input, and the adjustment of three key parameters (the effective light-use efficiency, the date of plant emergence, and the cumulative thermal unit between emergence and senescence). These three parameters were adjusted from estimates of green leaf area index derived from FORMOSAT-2 images.

The SAFY model was used to drive a soil water balance that was described and evaluated in [Duchemin et al. \(2005\)](#). The model calculates soil evaporation and plant transpiration using a dual-crop coefficient approach (adapted from FAO paper #56, see [Allen et al. 1998](#), [Allen 2000](#)). Three layers are implemented to describe soil water transfers: (1) a 5-cm depth top layer, (2) a root zone, which progressively increases to reach maximal value at the end of the vegetative phase, (3) a deeper layer, until 1m, that plays the role of a bank of the water

accumulated during the agricultural (rainy) season. The model simulates soil water contents within these 3 layers with reference evapotranspiration and water supply (rainfall and irrigation) as inputs. The topsoil humidity (HM1) is used together with GLA to analyse the spatio-temporal variations of radar data.

Simulations were performed at a daily time step on 69 fields where irrigation data are available. The outputs were evaluated on the 8 test fields where Green Leaf Area index (GLA) and Dry Aerial Mass (DAM) were measured at ground.

III. Results and discursions

III.1 Typical time courses of NDVI and $\sigma_{HH/VV}^0$

As a first analysis, the Normalised Difference Vegetation Index (NDVI) and the ratio of HH to VV backscattering coefficient ($\sigma_{HH/VV}^0$) were compared between three field with different vegetation types: young olive trees with a vegetation fraction cover measured at field to about 30%, fallow and wheat (fig. 1). For the three fields, NDVI and $\sigma_{HH/VV}^0$ follow comparable time courses:

- Olive trees: both NDVI and $\sigma_{HH/VV}^0$ remains rather stable, around -1db and 0.35, respectively. This stability is explained by the fact that olive tree didn't vary significantly in 6 months. The small peaks observed on March and April (DO2Y 440 to 480 in fig.1) are due to the weeds that growth between trees during this period.
- Fallow: at the beginning of the season, $\sigma_{HH/VV}^0$ is around -1.5db and NDVI is about 0.15. These values are characteristic of bare soils. $\sigma_{HH/VV}^0$ and NDVI progressively increase after the first significant rainfall to reach their maximum values at the beginning of April (DO2Y=470 in fig.1), then decrease with the vegetation senescence.
- Wheat: the most important temporal variations of $\sigma_{HH/VV}^0$ and NDVI are observed for the wheat field. Both indices clearly describe the cycle of wheat plants: they displays minimum values in November-December (at the sowing period), then a rapid increase to maximum values mid-March (DO2Y=450 in fig.1) when plant reaches maturity, and a final decrease until May at the harvesting time.

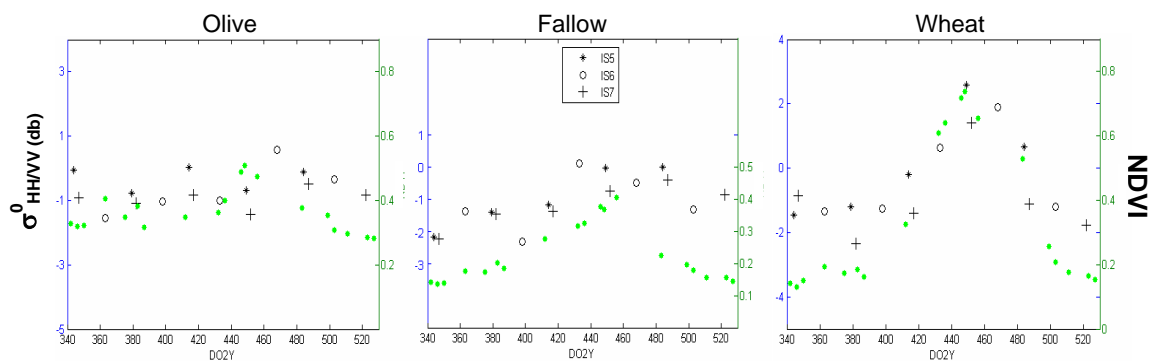


Figure 1. Time courses of $\sigma_{HH/VV}^0$ and NDVI for 3 vegetation types: olive trees, fallow and wheat. Blacks symbols correspond to ASAR observation (stars, circles and plus for incidence angles IS5, IS6 and IS7). Green dots represent NDVI. DO2Y is day since 1/1/05

These first findings illustrate the potential of both optical and radar images to get land use maps using classification method (Mróz and Ciołkowska 2004, Holah 2005) as well as to

monitor the vegetation dynamics. However, there is much scatter on ASAR than on FORMOSAT-2 data, due to differences in incidence angles and the high sensitivity of the radar response to surface characteristics that experience a large spatio-temporal variability (topsoil moisture, surface roughness).

III.2 Inversion of Green Leaf Area index from FORMOSAT-2 data

The two vegetation indices (RVI and NDVI) derived from FORMOSAT-2 data were tested to estimate Green Leaf Area index (GLA). For this purpose, we compared GLA measured at ground on 24 plots (3 samples of 1 m² for each of the 8 fields) to the values of the vegetation indices of the pixels which includes the plots. The measurements, which were performed at end of March (March 20 to 24, 2006), range from 1.2 to 6.2 m²/m² at this time. They were compared to NDVI and RVI indices derived from the FORMOSAT-2 image acquired on March 24. The result shows that the RVI performs the best to fit GLA. The scatterplot and the GLA-RVI relationship are presented in figure 2. The root mean square error between the measured GLA and those derived from the FORMOSAT-2 image using this relationship is about 0.8 m²/m² (relative error of 25%). This error appears of the same order than that reported in other studies (e.g. [Weiss et al. 2004](#), [Duchemin et al. 2006](#)).

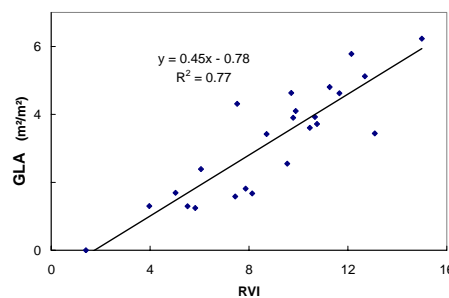


Figure 2. GLA-RVI scatterplot

III.3 Time courses of Green Leaf Area index (GLA) and Dry Aerial Mass (DAM)

In figure 3, we present the comparison between the green leaf area index simulated by SAFY, that retrieved from the 26 FORMOSAT images all along the agricultural season and that measured on each of the 8 test fields. This figure shows the capability of the model to accurately simulate the time courses of green leaf area index, despite a slight overestimation at the very beginning of the agricultural season. The model also appears able to simulate GLA spatial variations: at the end of the vegetative phase (end of March), the green leaf area index measured at field varies between 2.2 and 6.2 m²/m², and the root mean square error between measurements and simulations is 0.85 m²/m² (relative error of about 20%).

In figure 4, we compare the dry aerial biomass simulated and that measured on each of the 8 test fields. At the end of vegetative phase (end of March), the biomass measured at field varies from 0.2 to 0.75 kg/m², and the root mean square error (rmse) between measurements and simulations is about 0.1 kg/m² (relative error of about 20%). At the end of the season, the accuracy of the model decreases: measurements range between 0.6 and 1.3 kg/m², the rmse is 0.5 kg/m² (relative error of about 60%).

These results confirm the performance of the SAFY model to simulate the spatio-temporal dynamics of wheat canopies, especially during the vegetative period.

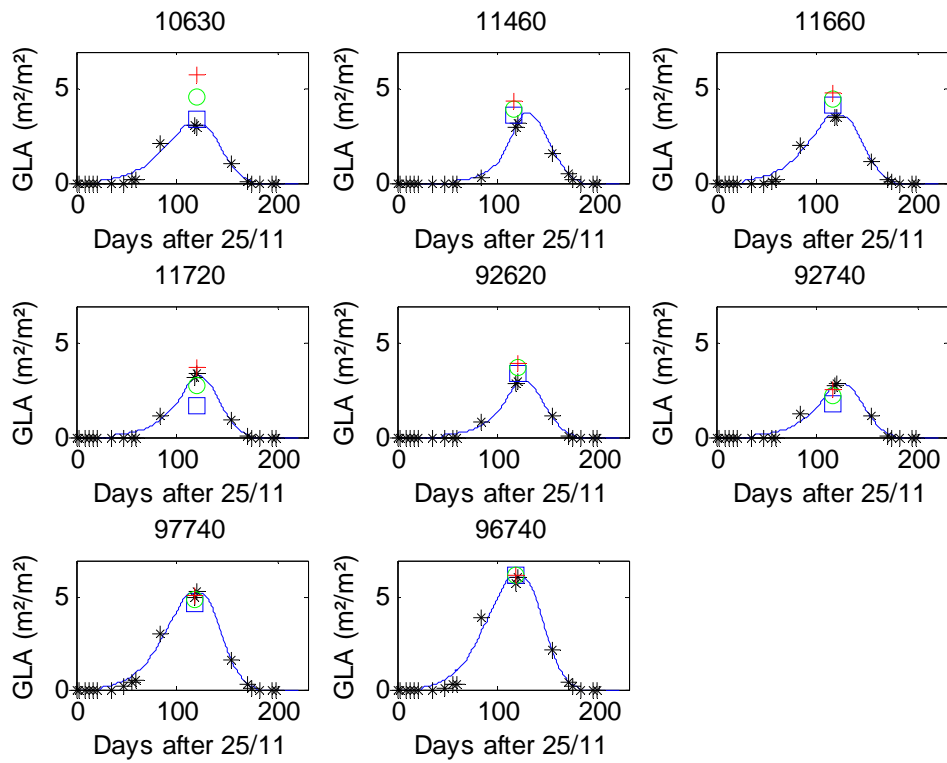


Figure 3. Green leaf area index (GLA) simulated by the SAFY model (lines), derived from FORMOSAT-2 data (black stars) and measured at field (blue squares, green circles and red plus correspond to minimal, mean and maximal values, respectively)

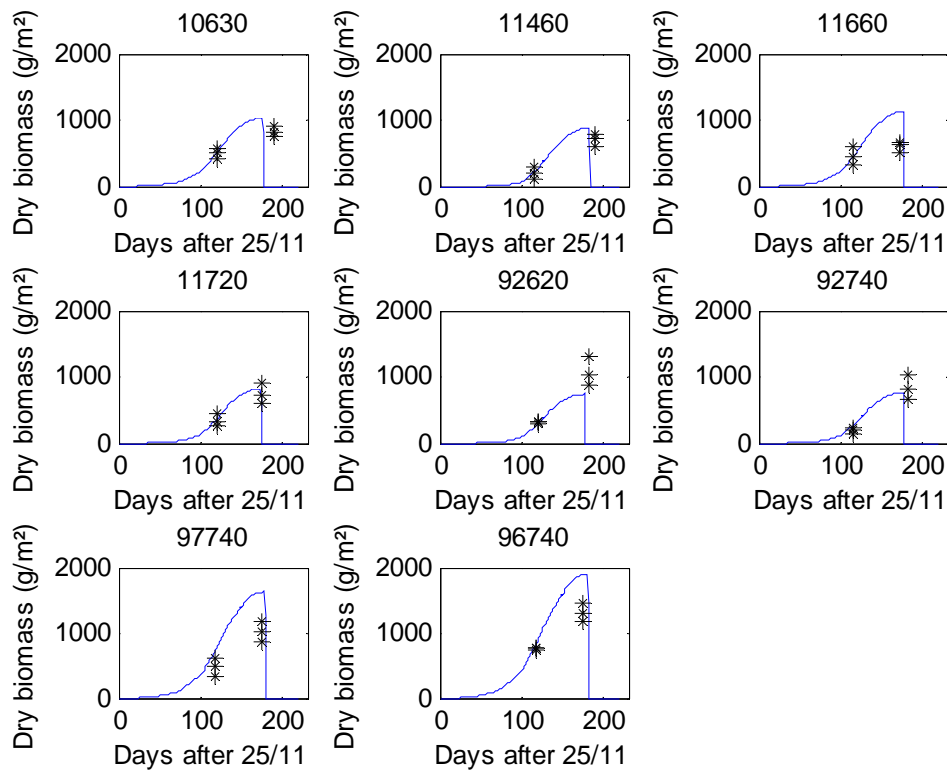


Figure 4. Simulated (lines) and observed (stars: min, max and average values are presented) dry aerial biomass

III.4 Potential and limits of ASAR data for the monitoring of irrigated wheat crops

In this section, the simulated soil/plant conditions were used to analyse the space time variations of the ratio of HH to VV backscattering coefficients ($\sigma_{HH/VV}^0$) derived from ASAR images. The sensitivity of HH/VV backscatter to wheat canopy biomass is caused by the differential attenuation of horizontally and vertically polarized electromagnetic waves that propagate through a medium with vertical structure (Bracaglia et al. 1995; Picard et al., 2003).

Simulations of green leaf area index (GLA) and top soil humidity (HM1) are available on the 69 fields where irrigation data are known. ASAR data were averaged to one value for each field to minimize the speckle effect. Field-averaged $\sigma_{HH/VV}^0$ are compared to GLA for the three incidence angles (IS5, IS6 and IS7) in figures 5, 6, 7, where the distribution of topsoil moisture is also plotted. GLA is used as an indicator as the total vegetation water content, which is believed correct during the vegetation phase when simulations are the most accurate and when the vegetation water content does not experience large variations.

At the very beginning of the agricultural season (December), $\sigma_{HH/VV}^0$ varies a lot, from -2 db to 1 d. There is no clear impact of incidence angles and soil moisture on $\sigma_{HH/VV}^0$ (compare top-figures 5 to 7). The range of variation of $\sigma_{HH/VV}^0$ is still large even when the vegetation recovering is null and when the top-soil moisture is rather homogeneous (see top-figures 5 and 7). The explanation lies in surface roughness. Indeed, there are 3 categories of surface states at this period of year, depending on agricultural practices: fields may be harrowed (sown or prepared to be sown), ploughed in depth (but not yet harrowed), or smooth (not ploughed neither harrowed). These conditions result in large variation of surface roughness, with root mean square error associated to surface height profiles from about 0.5 to 6 cm according to the classification of Davidson et al. (2000).

In January, a large scatter on $\sigma_{HH/VV}^0$ is also observed, despite the soil conditions are homogeneous, either dry (14/01/06, in fig.5) or wet after heavy rainfall (17/01/06, in fig.7). This scattering prevents the use of ASAR data to monitor the vegetation just after emergence. This indicates that there is still a large heterogeneity of surface roughness between fields, even after sowing.

Relationship between GLA and $\sigma_{HH/VV}^0$ can be noticed for the three images acquired in February. On the first image (02/02/06, IS6, fig.6-middle), there is a large scatter on $\sigma_{HH/VV}^0$, despite soils are homogeneously wet. On the second one (18/02/06, IS5, fig.5-middle), there is also a large scatter on $\sigma_{HH/VV}^0$, which can be due to heterogeneity of topsoil moisture as well as surface roughness. The relationship is only clear for the third image (21/02/06, IS7, fig.7-middle), which have been acquired just after an important rainfall that saturates top-soil moisture. On this scatterplot, ones can see that $\sigma_{HH/VV}^0$ saturates when GLA is larger than 1.5. These scatterplots appear consistent with those of other experiments (e.g. Mattia et al. 2003, 2005), though the saturation seems more intense in the conditions that prevail in this study.

From March to May, there is no clear relationship between GLA and $\sigma_{HH/VV}^0$. The possible explanations are the following: (1) as previously discussed, $\sigma_{HH/VV}^0$ saturates at high GLA values; (2) this period corresponds to the maximal heterogeneity of topsoil moisture because of irrigation, but the sensitivity of the radar response to surface soil moisture content is substantially decreased at high GLA values; (3) the radar response is also due to interaction with ears, in addition of leaves and stems; (4) variations in vegetation water content, which are not accounted for here, becomes larger at the end of the agricultural season.

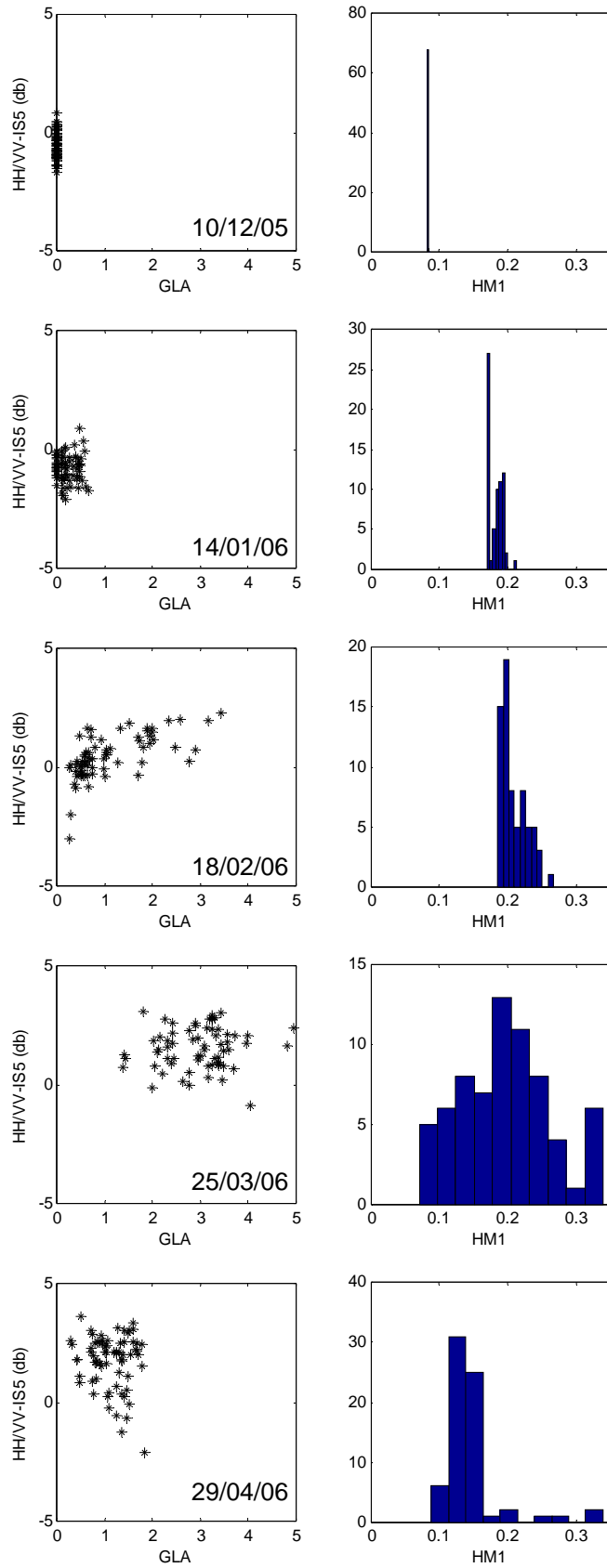


Figure 5. $\sigma_{HH/VV}^0$ - GLA scatterplot (incidence angle 5)

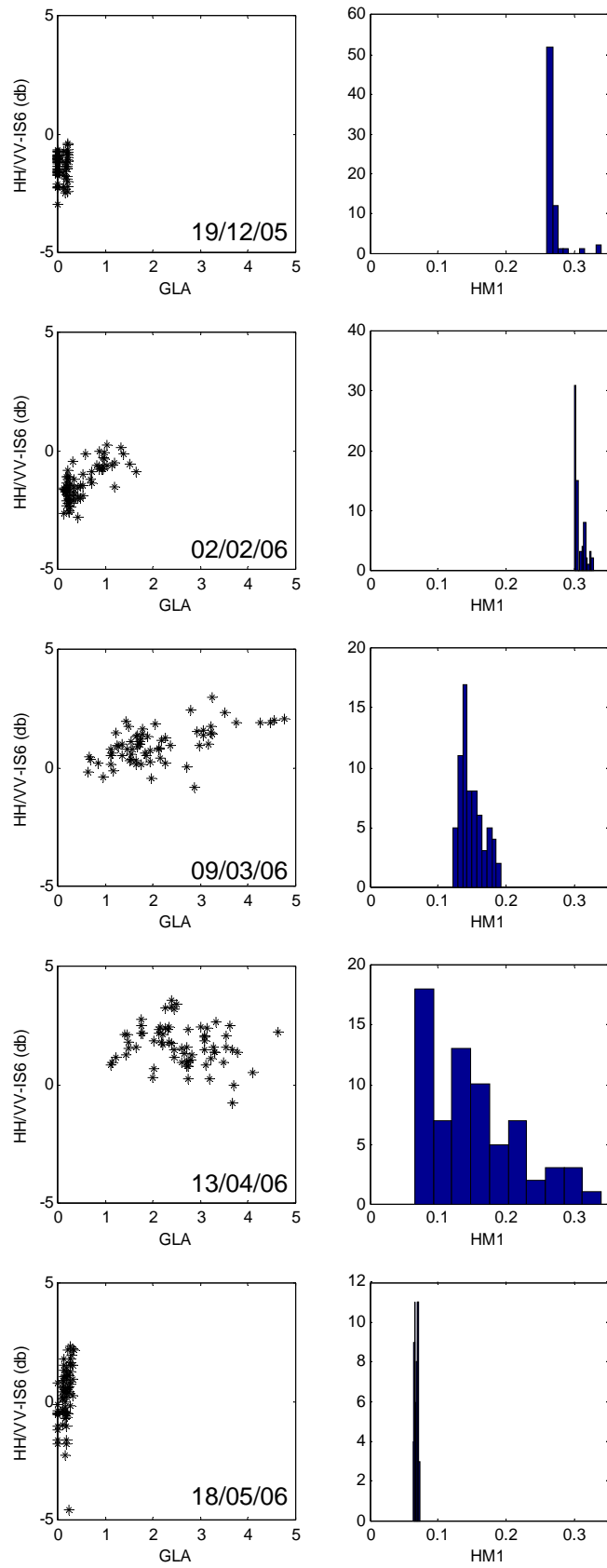


Figure 6. $\sigma_{HH/VV}^0$ - GLA scatterplot (incidence angle 6)

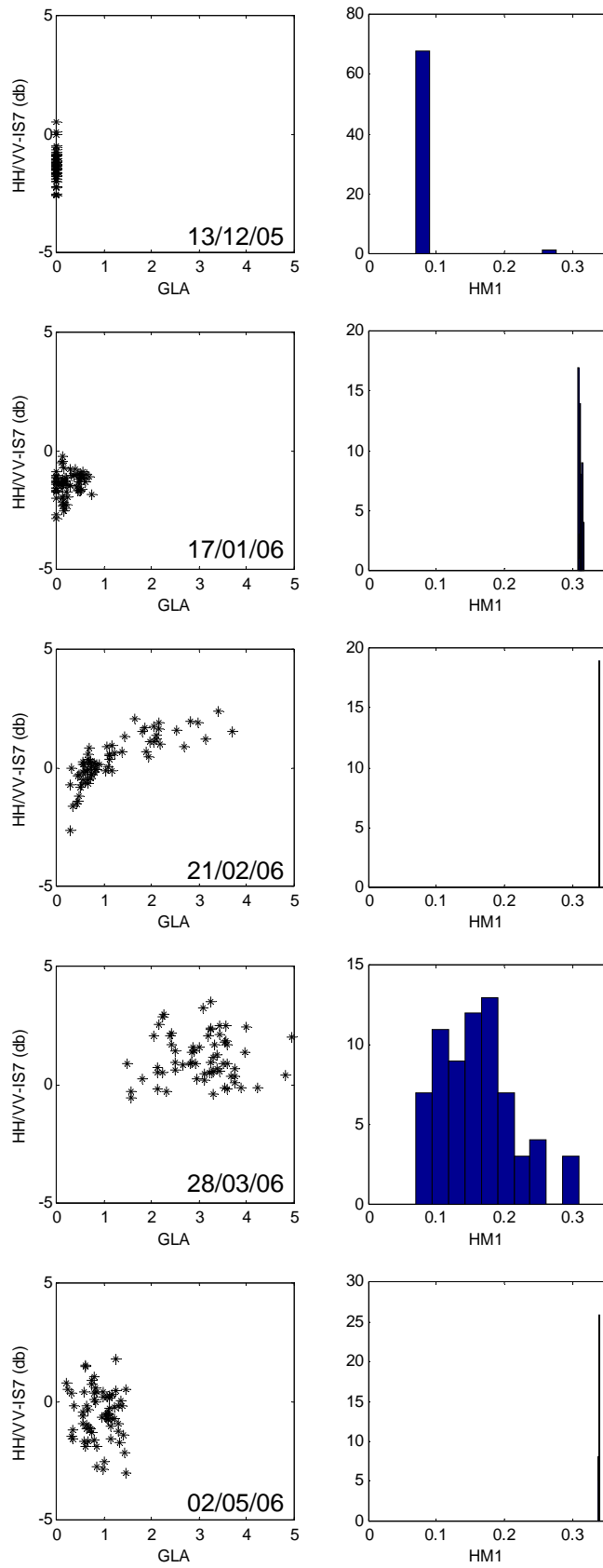


Figure 7. $\sigma_{HH/VV}^0 / \text{GLA}$ scatterplot (incidence angle 7)

IV. Conclusions

The main conclusions of this research are threefold:

(A) The accuracy of the inversion of wheat canopy biophysical variables (green leaf area index) from vegetation indices derived from FORMOSAT-2 images is around 25%. The inversion is more accurate since directional effects are minimized (constant viewing angles). This makes possible the use of non-normalised indices (e.g. RVI instead of NDVI).

(B) The SAFY model appears as a good interpolator of the green leaf area index. It also accurately simulates the time courses of dry aerial mass during the vegetative phase (relative error of about 20% on these two variables at the peak of greenness). These results appear correct given the heterogeneity of canopies in the study area (sowing period from the end of November to the beginning of January, grain yield from 1 to 4 t/ha).

(C) In the conditions that prevail in this study, the sensitivity of ASAR data to the vegetation density appears very low. It is in fact non-existent except at the tillering period and when the soil conditions are homogeneous, after heavy rainfall. Only upon these (very restrictive) conditions, ASAR data can serve as a substitute to optical data for the monitoring of vegetation canopies.

Acknowledgments

This study was conducted within the framework of the Sud-Med project coordinated by IRD/CESBIO and University of Marrakech (UCAM, université Cadi Ayyad de Marrakech). In addition to IRD, this research has been supported by the PLEIADeS project of the European Commission (Contract 4 GOCE 037095), the “*Programme d'Action Intégrée du Comité Mixte Interuniversitaire Franco-Marocain*” (PAI Volubilis 06/148), and the French “*Programme National de Télédétection Spatiale*” (PNTS). Rachid Hadria was supported by a postdoc fellowship of French National Research Center (CNRS, *Centre National de Recherche Scientifique*). We acknowledge NSPO, SPOT-Image and the French National Space Agency (CNES, Centre National d'Etudes Spatiales) for the delivery and the processing FORMOSAT-2 images. ENVISAT/ASAR images were provided by ESA as part of a “Category-1 data use” proposal (AOE443, PI: Dr. E. Mougin). The authors are indebted to the staff and the directors of Sud-Med regional partners, and especially ORMVAH (Office Régional de Mise en Valeur Agricole du Haouz) for their collaboration in field survey.

References

- Allen, R.G., Pereira, L.S., Raes, D., Smith, M., 1998. Crop Evapotranspiration-Guidelines for Computing Crop Water Requirements, Irrigation and Drain, Paper No. 56. FAO, Rome, Italy, 300 pp.
- Allen, R.G., 2000. Using the FAO-56 dual crop coefficient method over an irrigated region as part of an evapotranspiration intercomparison study. *J. Hydrol.* 229, 27–41.
- Bastiaanssen, W.G.M., Allen, R.G., Droogers, P., D'Urso, G., Steduto, P., 2007. Twenty-five years modeling irrigated and drained soils: State of the art. *Agricultural Water Management.* 92, 111–125.
- Benhadj I., Hadria R., Duchemin B., Simonneaux V., Le Page M., Mougnot B., Hagolle O., Dedieu G. High spatial and temporal resolution FORMOSAT-2 images: first results and

perspectives for land cover mapping of semi-arid areas (Marrakech/Al Haouz plain). Fourth International Workshop on the Analysis of Multi-temporal Remote Sensing Images 18-20 July 2007, Leuven, Belgique.

Boote, K.J., Jones, J.W. and Pickering, N.B., 1996. Potential uses and limitations of crop models. *Agronomy Journal*. 88, 704–716.

Brown, Sarah C. M., Quegan, S., Morrison, K., Bennett, John C., Cookmartin, G., 2003, High-Resolution Measurements of Scattering in Wheat Canopies—Implications for Crop Parameter Retrieval; *IEEE IEEE transactions on geoscience and remote sensing* 41:1602:1610.

Chebouni A., Escadafal R., Duchemin B., Boulet G., Simonneaux V., Dedieu G., Mougenot B., Khabba S., Kharrou M.H., Maisongrande P., Merlin O., Chaponnière A., Ezzahar J., Er-Raki S., Hoedjes J., Hadria R., Abourida A., Cheggour A., Raïbi F., Boudhar A., Benhadj I., Hanich L., Benkaddour A., Guemouria N., Chebouni A.H., Lahrouni A., Oliosio A., Jacob F., Williams D.G., Sobrino J. (2007). An integrated modelling and remote sensing approach for hydrological study in arid and semi-arid regions: the SUDMED Program. *International Journal of Remote Sensing*, in press.

Davidson, M., Le Toan, T., Mattia, F., Satalino, G., Manninen, T., Verhoef, N. and Borgeaud, M., 2000. On the characterization of Agricultural Soil roughness for radar remote sensing studies. *IEEE Geoscience and Remote Sensing*, 38 (2): 630-640.

Duchemin B., G. Boulet, P. Maisongrande, I. Benhadj, R. Hadria, S. Khabba, Chehbouni A., Oliosio A. Un modèle simplifié pour l'estimation du bilan hydrique et du rendement de cultures céréalières en milieu semi-aride. Deuxième Congrès Méditerranéen « Ressources en Eau dans le Bassin Méditerranéen », Marrakech (Maroc), 14-17 Novembre 2005.

Duchemin, B., Hadria, R., Er-Raki, S., Boulet, G., Maisongrande, P., Chehbouni, A., Escadafal, R., Ezzahar, J., Hoedjes, J., Karroui, H., Khabba, S., Mougenot, B., Oliosio, A., Rodriguez, J-C. and Simonneaux, V., 2006. Monitoring wheat phenology and irrigation in Center of Morocco : on the use of relationship between evapotranspiration, crops coefficients, leaf area index and remotely-sensed vegetation indices. *Agricultural and Water Management*. 79, 1–27.

Duchemin B., Maisongrande P., Boulet G, Benhadj. I (2008a). A simple algorithm for yield estimates: calibration and evaluation for semi-arid irrigated winter wheat monitored with ground-based remotely-sensed data. *Environmental Modelling and Software* 23:876-892.

Duchemin B., Hagolle O., Mougenot B., Simonneaux V., Benhadj I., Hadria R., Ezzahar J., Hoedjes J., Khabba S., Kharrou M.H., Boulet G., Dedieu G., Er-Raki S., Escadafal R., Oliosio A., Chehbouni A. (2008b). "Agrometeorological study of semi-arid areas: an experiment for analysing the potential of FORMOSAT-2 time series of images in the Marrakech plain". *International Journal of Remote Sensing*, in press.

Er-Raki S., Chehbouni A., Guemouria N., Duchemin B., Ezzahar J., Hadria R. (2007). "Combining FAO-56 model and ground-based remote sensing to estimate water consumptions of wheat crops in a semi-arid region". *Agricultural water management* 87:41–54.

Faivre, R., Leenhardt, D., Voltz, M., Benoît, M., Papy, F., Dedieu, G. and Wallach, D., 2004. Spatialising crop models. *Agronomie*. 24, 205-217.

FAO/IPTRID 1999. Poverty reduction and irrigated agriculture, by Hasnip N., Vincent L., Hussein K. Issue Paper 1. January 1999. FAO. Rome. <http://www.fao.org/docrep/005/X1000E/X1000E00.HTM>

- Guérif, M. and Duke, C., 2000. Adjustment procedures of a crop model to the site specific characteristics of soil and crop using remote sensing data assimilation. *Agriculture, Ecosystems and Environment*. 81, 57–69.
- Hadria, R., Duchemin, B., Lahrouni, A., Khabba, S., Er-Raki, S., Dedieu, G. and Chehbouni, A., 2006. Monitoring of irrigated wheat in a semi-arid climate using crop modelling and remote sensing data: Impact of satellite revisit time frequency. *International Journal of Remote Sensing*. 27, 1093-1117.
- Hadria R., Khabba S., Lahrouni A., Duchemin B., Chehbouni A., Carriou J., Ouzzine L. (2007). "Calibration and Validation of the STICS Crop Model for Managing Wheat Irrigation in the Semi-Arid Marrakech/Al Haouz Plain". *Arabian Journal for Science and Engineering* 32:87:101. (special issue potential water challenges and solutions in the new millennium in arid regions, http://www.kfupm.edu.sa/publications/ajse/articles/321C_P.07.pdf).
- Hagolle O., Dedieu G., Mougenot B., Debaecker V., Duchemin B., Meygret A. (2008). Correction of aerosol effects on multi-temporal images acquired with constant viewing angles: application to Formosat-2 images. *Remote Sensing of Environment* 112:1689-1701.
- Holah, N., 2005, Potentiel des nouveaux capteurs radar multipolarisation et polarimétrique pour la caractérisation des états de surface en milieu agricole ; thèse de doctorat, UNIVERSITE D'ORLEANS ; 247pages.
- Houlès, V., Guérif, M., Bruno Mary, B., 2007. Elaboration of a nitrogen nutrition indicator for winter wheat based on leaf area index and chlorophyll content for making nitrogen recommendations. *Europ. J. Agronomy*. 27, 1–11.
- Le Toan, T., Ribbes, F., Wang, L.-F., Floury, N., Ding, K.-H., Kong, J. A., Fujita, M. and Kurosu, T., 1997. Rice Crop Mapping and Monitoring Using ERS-1 Data Based on Experiment and Modeling Results, *IEEE Trans. on Geoscience & Remote Sensing* 35: 41-56.
- Lobell, D.B., Asner, G.P., Ortiz-Monasterio, J.I., Benning, T.L., 2003. Remote sensing of regional crop production in the Yaqui Valley, Mexico: estimates and uncertainties. *Agriculture, Ecosystems and Environment*. 94, 205–220.
- Lopes, A., Nezry, E., Touzi, R. and Laur, H. ,1993. Structure detection and statistical adaptative speckle filtering in SAR images. *Int. J. Remote Sensing*, 14: 1735–1758.
- Mattia, F., Le Toan, T., Picard, G., Posa, F.I., D'Alessio, A., Notarnicola, C., Gatti, A.M., Rinaldi, M., Satalino, G. and Pasquariello, G., 2003, Multitemporal C-Band Radar Measurements on Wheat Fields; *IEEE transactions on geoscience and remote sensing*, vol. 41, n°. 7, 1551- 1560.
- Mattia F., L. Dente, G. Satalino, T. Le Toan (2005) Sensitivity of ASAR AP data to wheat crop parameters, *Proc. of 2004 ENVISAT & ERS Symposium*, Salzburg, Austria, ESA SP-572, CDROM, 2005.
- Mo X., Liu S., Lin Z., Xu Y., Xiang Y., McVicar T.R. (2005). Prediction of crop yield, water consumption and water use efficiency with a SVAT-crop growth model using remotely sensed data on the North China Plain. *Ecological Modelling* 183:301-322.
- Moran, M. S., Hymer, D. C., Qi, J. and Kerr, Y., 2002. Comparison of ERS-2 SAR and Landsat TM imagery for monitoring agricultural crop and soil conditions. *Remote Sensing of Environment*, 79: 243– 252.
- Moulin, S., Bondeau, A. and Delécolle, R., 1998. Combining agricultural crop models and satellite observations from field to regional scales. *International Journal of Remote Sensing*. 19, 1021–1036.

- Mróz, M. and Ciołkowska, M., 2004, Synergetic use of ENVISAT-1/ ASAR IMG / APG data and optical SPOT XS/XI data for land cover and agricultural crops mapping; Proc. of 2004 Envisat & ERS Symposium, Salzburg, Austria 6-10 Sept. 2004 (ESA SP-572, April 2005).
- Oliosio, A., Inoue, Y., Ortega-Farias, S., Demarty, J., Wigneron, J-P., Braud, I., Jacob, F., Lecharpentier, P., Ottlé, C., Calvet, J.-C. and Brisson, N., 2005. Future directions for advanced evapotranspiration modeling: assimilation of remote sensing data into crop simulation models and SVAT models. *Irrigation and Drainage Systems*. 19, 377-412.
- Ortiz-Monasterio, J.I., Lobell, D.B., 2007. Remote sensing assessment of regional yield losses due to sub-optimal planting dates and fallow period weed management. *Field Crops Research*. 101, 80–87.
- Quegan, S. and J. Yu, J., 2001. Filtering of Multichannel SAR Images. *IEEE Transactions on Geoscience and Remote Sensing*, 39: 2373-2379.
- Rahman, H., Dedieu G., 1994, SMAC: a simplified method for the atmospheric correction of satellite measurements in the solar spectrum. *International Journal of Remote Sensing* 15, 123-143.
- Rouse, J. W., Haas, R. H., Schell, J. A., Deering, D. W., and Harlan, J. C. (1974) "Monitoring the vernal advancement and retrogradation (greenwave effect) of natural vegetation", NASA/GSFC Type III Final Report_, Greenbelt, Md. 371 p.
- Scotford I.M., P.C.H. Miller (2005). Applications of Spectral Reflectance Techniques in Northern European Cereal Production: A Review. *Biosystems Engineering* 90:235–250.
- Tasumi, M., Allen, R.G., 2007. Satellite-based ET mapping to assess variation in ET with timing of crop development. *Agricultural Water Management*. 88, 54–62.
- Weiss M., Baret F., Smith G.J., Jonckheere I., Coppin P (2004). Review of methods for in situ leaf area index (LAI) determination: Part II. Estimation of LAI, errors and sampling. *Agricultural and Forest Meteorology*, 121:37-53.